

AD-A113 805

AEROSPACE CORP EL SEGUNDO CA MATERIALS SCIENCES LAB
PITCH FRACTIONATION.(U)

F/G 7/4

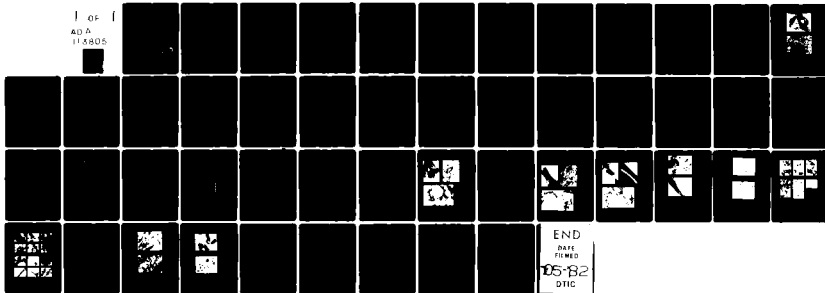
DEC 81 V L WEINBERG, J L WHITE
TR-0082(2935-02)-1

F04701-81-C-0082
NL

UNCLASSIFIED

SD-TR-81-90

1 OF 1
AD A
114805



12

AD A113805

Pitch Fractionation

V. L. WEINBERG and J. L. WHITE
Materials Sciences Laboratory
Laboratory Operations
The Aerospace Corporation
El Segundo, Calif. 90245

15 December 1981

APPROVED FOR PUBLIC RELEASE;
DISTRIBUTION UNLIMITED

Prepared for
SPACE DIVISION
AIR FORCE SYSTEMS COMMAND
Los Angeles Air Force Station
P.O. Box 92960, Worldway Postal Center
Los Angeles, Calif. 90009

DTIC FILE COPY

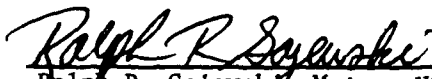
DTIC
ELECTE
APR 26 1982
H


82 12 022

This report was submitted by The Aerospace Corporation, El Segundo, CA 90245, under Contract No. F04701-81-C-0082 with the Space Division, Deputy for Technology, P.O. Box 92960, Worldway Postal Center, Los Angeles, CA 90009. It was reviewed and approved for The Aerospace Corporation by W. C. Riley, Director, Materials Sciences Laboratory. Major Ralph R. Gajewski, SD/YLXT, was the project officer for the Mission Oriented Investigation and Experimentation Program.

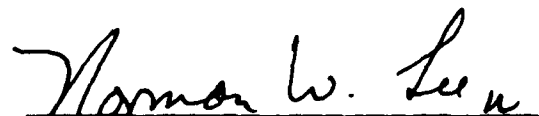
This report has been reviewed by the Public Affairs Office (PAS) and is releasable to the National Technical Information Service (NTIS). At NTIS, it will be available to the general public, including foreign nations.

This technical report has been reviewed and is approved for publication. Publication of this report does not constitute Air Force approval of the report's findings or conclusions. It is published only for the exchange and stimulation of ideas.


Ralph R. Gajewski, Major, USAF
Project Officer


Florian P. Meinhardt, Lt Col, USAF
Director of Advanced Space
Development

FOR THE COMMANDER


Norman W. Lee, Jr., Colonel, USAF
Deputy for Technology

SECURITY CLASSIFICATION OF THIS PAGE (When Data Entered)

DD FORM 1473
(FACSIMILE)

SECURITY CLASSIFICATION OF THIS PAGE (When Data Entered)

UNCLASSIFIED

SECURITY CLASSIFICATION OF THIS PAGE(When Data Entered)

19. KEY WORDS (Continued)

20. ABSTRACT (Continued)

fraction increased, the pyrolysis yield and bloating increased, and the microstructure of the coke became finer until glassy microconstituents were formed in the deepest fractions.

UNCLASSIFIED

SECURITY CLASSIFICATION OF THIS PAGE(When Data Entered)

CONTENTS

I.	INTRODUCTION.....	7
II.	FRACTIONATION.....	9
III.	PYROLYSIS OF PITCH FRACTIONS.....	27
IV.	MICROSTRUCTURES OF PYROLYZED FRACTIONS.....	33
	A. Fractionation Series AG 162-5.....	33
	B. Fractionation Series AG 162-7.....	35
V.	DISCUSSION.....	45
	REFERENCES	47



Accession For	
NTIS GRA&I	<input checked="" type="checkbox"/>
DTIC TAB	<input type="checkbox"/>
Unannounced	<input type="checkbox"/>
Justification	
By _____	
Distribution/	
Availability Codes	
Avail and/or	
Dist	Special
A	

TABLES

1.	Starting Materials for Pitch Fractionation.....	10
2.	Solvents for Pitch Extraction.....	12
3.	Fractionation of A240 Petroleum Pitch AG 12-34.....	17
4.	Fractionation of Pyrolyzed Pitch AG 164A.....	18
5.	Fractionation of Mesophase Pitch AG 164B.....	19
6.	Fractionation of Mesophase Pitch AG 164B.....	20
7.	Comparison of Aromatic and Aliphatic Infrared Absorption Peaks.....	24

FIGURES

1.	Mesophase Pitch AG 164B.....	11
2.	Fractionation Sequence AG 162-7.....	13
3.	Solvent Fractionation Experiments.....	15
4.	Fourier Transform Infrared Spectra for A240 Petroleum Pitch AG 12-34 and Mesophase Pitch AG 164B.....	21
5.	Fourier Transform Infrared Spectra.....	23
6.	Relative Aromaticities of Pitch Fractions as a Function of H/C Ratio.....	25
7.	Pyrolysis Cell.....	28
8.	Coking Yield and Bloating Behavior of Fractionation Sequence AG 162-4.....	29
9.	Coking Yield and Bloating Behavior of Fractionation Sequence AG 162-5.....	30
10.	Coking Yield and Bloating Behavior of Fractionation Sequence AG 162-6.....	31
11.	Coking Yield and Bloating Behavior of Fractionation Sequence AG 162-7.....	32
12.	Microstructure of Coke Formed by Pyrolysis of Pitch AG 164A.....	34
13.	Microstructure of Coke Formed by Pyrolysis of Hexane Fraction of Fractionation Series AG 162-5.....	36
14.	Microstructure of Coke Formed by Pyrolysis of Chloroform Fraction of Fractionation Series AG 162-5.....	37
15.	Microstructure of Coke Formed by Pyrolysis of Pyridine Fraction of Fractionation Series AG 162-5.....	38
16.	Microstructure of Coke Formed by Pyrolysis of Pyridine-Insoluble Fraction of Fractionation Series AG 162-5.....	39
17.	Microstructure of Cokes Produced by Pyrolysis of Fractions from Fractionation Series AG 162-7.....	40
18.	Microstructure of Cokes Produced by Pyrolysis of Fractions from Fractionation Series AG 162-7.....	41

FIGURES (Continued)

19. Microstructure of Coke Produced by Pyrolysis of Quinoline
Fraction from Fractionation Series AG 162-7..... 43
20. Microstructure of Coke Produced by Pyrolysis of Quinoline-
Insoluble Fraction from Fractionation Series AG 162-7..... 44

I. INTRODUCTION

From a chemical viewpoint, the petroleum and coal-tar pitches employed in the fabrication of carbon-matrix carbon-fiber-reinforced composites are complex substances consisting for the most part of a large number of polynuclear aromatic hydrocarbons and heterocyclic compounds.^{1,2} Pyrolysis of these materials usually proceeds through a liquid-crystal (mesophase) transformation.^{3,4} The mesophase morphologies formed during this transition have been shown to be the essential forerunners for the microstructures found in the final carbon or graphite products.⁵ However it is not presently possible to trace back beyond the mesophase transformation to state precisely which precursor molecules, or combinations of molecules, are the most effective components for such pitch applications as composite impregnants or graphite binders.

In the present investigation we are seeking practical ways to improve pitches for demanding applications by subjecting commercial pitches to thermal treatment and solvent fractionation and examining the pyrolysis behavior of each fraction at room pressure and at the pressure levels involved in fabricating carbon-carbon composites. The initial work described in this report^{*} was limited to one petroleum pitch (Ashland A240) at three levels of thermal treatment. The primary focus was on finding a series of sequential extractions with increasingly aggressive solvents to split the pitches into at least five roughly equal fractions. Although it is recognized that the insoluble particles characteristic of coal-tar pitches may play important roles in the pyrolysis behavior,⁶ the insoluble-free petroleum pitch was chosen for the initial work to avoid having to deal with insoluble particles while developing the extraction sequence.

^{*}The work described in this report was supported by the U.S. Air Force under Space Division Contract No. FO4701-81-C-0082 (MOIE Program) for fiscal year 1982. The application of pitch fractionation to the development of improved composite matrices is currently supported by the Naval Surface Weapons Center (SMMT Program).

II. FRACTIONATION

The starting material for the fractionation experiments was Ashland A240 petroleum pitch in three stages of thermal treatment: as-received, after pyrolysis to 360°C, and after pyrolysis to 408°C to produce a mesophase pitch. The thermal treatments were applied to alter the molecular composition of the pitch by removing volatiles and cracking off aliphatic side-chains, and to intensify the cracking and polymerization reactions until a partially transformed mesophase pitch⁷ was formed. The chemical analyses of the three thermally treated starting materials are summarized in Table 1.

The pyrolysis to 360°C proved to be a gentle thermal treatment with 99% yield and little effect on the atomic hydrogen-to-carbon (H/C) ratio. This pyrolysis was conducted with the pitch in a number of 25-mm-diameter test tubes that fitted closely into holes in a copper block to ensure equivalent thermal conditions for all tubes. The block was heated at 13°C/hr to 360°C. Nitrogen gas, flushed gently through each tube, served as protective atmosphere.

The mesophase pitch was prepared by isothermal treatment in an aluminum vessel equipped with a rotary stirring device to maintain an emulsified structure during the mesophase transformation.⁷ The vessel was flushed with nitrogen. The 4-hr treatment at 408°C produced a yield of 88%. The microstructure is illustrated by Fig. 1. A point-counting technique was applied to 14 micrographs; the extent of transformation was found to be 50.6 (±6.5) vol%.

Some solvents considered for the sequential extractions are listed in Table 2 in order of their solubility parameters.^{8,9} This table includes an estimate by Riggs and Diefendorf¹⁰ for the range of solubility parameters that would apply to mesophase precipitating during the pyrolysis of various precursors. On this basis, the solvents are ordered in terms of increasingly aggressive solvent action for the constituents of a mesophase or near-mesophase pitch.

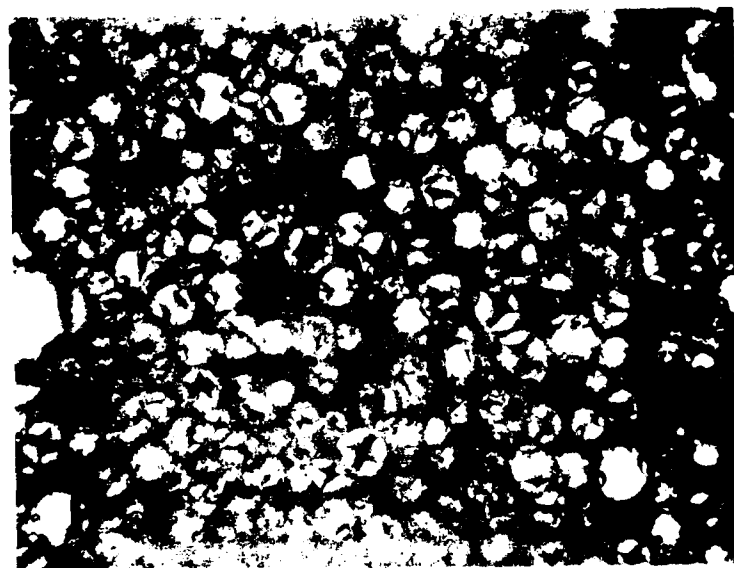
Table 1. Starting Materials for Pitch Fractionation

	Pitch Description with Lot Designation		
	A240 Pitch AG 12-34	Pyrolyzed Pitch AG 164A	Mesophase Pitch AG 164B
Thermal Treatment	None	13°C/hr to 360°C in 25-mm Glass Tubes	408°C for 5 hr in Stirred Reactor
Yield, wt%	-	99	88
Chemical Analyses, wt%			
Carbon	91.30	91.53	92.81
Hydrogen	5.36	5.39	5.13
Oxygen	1.52	0.98	0.37
Nitrogen	0.46	0.13	0.08
Sulfur	1.63	2.02	1.58
Ash	0.10	0.30	0.51
Atom Ratio, H/C	0.70	0.70	0.66
Coking Yield, wt%	61.6	66.7	71.5

Note: Chemical analyses by Huffman Laboratories, Inc., Wheatridge, Colorado.



500 μm



50 μm

Fig. 1. (a) Petro-
graph of the material
in the phase
region of the
phase diagram.

Table 2. Solvents for Pitch Extraction

Solvent	Solubility Parameter, (cal/cm ³) ^{1/2}	Boiling Point, °C	Reference
Pentane	7.0	36.1	8
Hexane	7.3	68.7	8
Cyclohexane	8.2	80.7	8
Toluene	8.9	110.6	8
Tetrahydrofuran (THF)	9.1	65.0	9
Chloroform	9.2	62.1	8
Benzene	9.2	80.1	8
Naphthalene	9.9	218.0	9
Pyridine	10.6	115.3	8
Quinoline	10.8	238.0	9
Carbonaceous Mesophase	10.5-12.5	-	10

Seven sequential extraction experiments were performed, based primarily on Soxhlet extraction and following closely the pattern given in Fig. 2 for the seventh extraction series. The results are summarized by the histograms in Fig. 3, which also define the various fractions described for brevity in this report as, for example, the benzene fraction. Thus, the third fraction of the seventh fractionation sequence, referred to as the benzene fraction, is seen to be defined more precisely as the hexane-insoluble, cyclohexane-insoluble, benzene-soluble fraction of the mesophase pitch.

The fractionation procedure was begun by reducing the dried starting material to particle sizes (-20 mesh) sufficiently fine to avoid excessive extraction times. Soxhlet extraction with hexane cannot be directly applied in the initial extraction because a tarry intermediate product clogs the filter and agglomerates the particles. Thus in the first step, the pitch particles (100 g) were slurried with 100 ml of benzene and then stirred into 4 liters of hexane (1 hr) to dissolve approximately one-half of the hexane-soluble fraction. The filter cake could then be subjected to conventional Soxhlet extraction. The fraction volumes desired for subsequent analysis and pyrolysis made it desirable to run two laboratory-scale Soxhlet extractors in parallel; each extractor used a cellulose extraction thimble (Whatman) 43 mm in diameter and a solvent volume of 0.6 liter. Each extraction was run in two stages of 2 days each to attain clarity in the solvent passing through the extraction thimble. The hexane-soluble fraction was then recovered by removing the hexane in a rotary evaporator.

Subsequent fractions were obtained by similar treatments applied sequentially with increasingly aggressive solvents, for example, cyclohexane, benzene, and pyridine. However, Soxhlet extraction with quinoline risks pitch decomposition reactions because of the high boiling point (238°C) of the solvent. The quinoline fraction was extracted by stirring the pyridine insolubles (10 g) into 1.5 liters of quinoline (freshly distilled) at 75°C for 0.5 hr. The quinoline-insoluble fraction was recovered by filtration, washing with acetone, and room-pressure distillation; changes in hydrogen and nitrogen content (relative to the pyridine and quinoline-insoluble fractions) suggested a tendency to reaction of the fraction despite the brief exposure at the boiling point of quinoline.

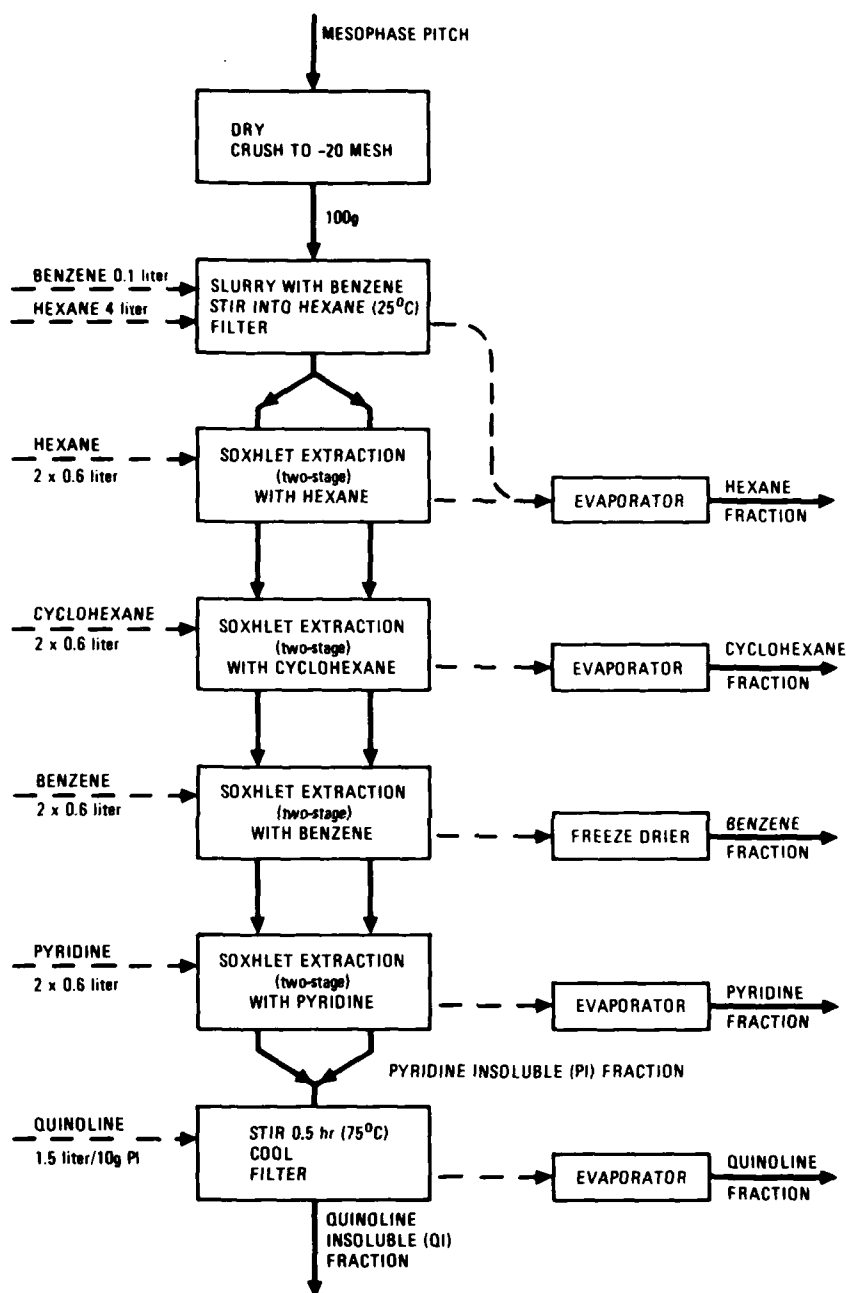


Fig. 2. Fractionation Sequence AG 162-7. Two paths are shown for the Soxhlet extractions because two Soxhlet extractors (600-ml capacity) were used in parallel to generate sufficient material for subsequent study.

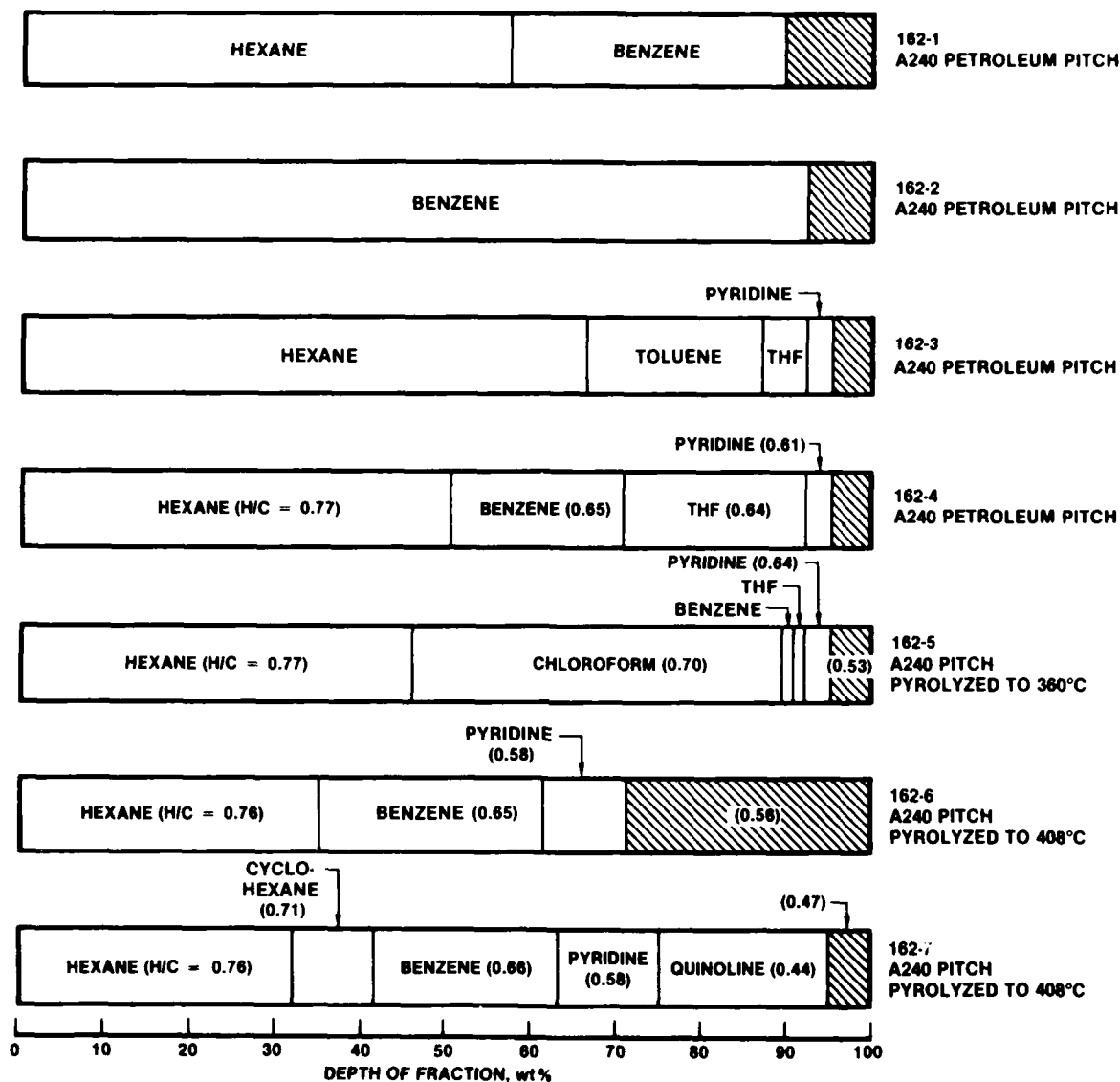


Fig. 3. Solvent Fractionation Experiments. Each histogram represents a sequential series of solvent extractions, commencing from the left and applied to the starting material described in the right-hand column. H/C ratios are indicated in parentheses for the latter four experiments.

All fractions, as well as the final insoluble materials, were dried under vacuum to constant weight to ensure removal of solvent.

The initial three fractionation sequences illustrated in Fig. 3 were primarily learning experiments to determine such experimental details as particle size, solvent volume, and extraction times. The goal of five soluble fractions, roughly equal in size, was achieved in the last fractionation sequence on the mesophase pitch. Analytical data for the last four fractionation sequences are presented in Tables 3 through 6; the elemental analyses were performed by Huffman Laboratories, Inc., Wheatridge, Colorado. H/C atom-ratios for the fractionation sequences are included in Fig. 3. This ratio decreases regularly with depth of fraction; one exception is the quinoline fraction of the last fractionation sequence where pyrolysis reactions during quinoline removal may have decreased the hydrogen content. In general, the H/C ratio remains fixed for a given solvent fraction over the range of three thermal treatments for the starting material.

The starting materials and the pitch fractions from the last fractionation sequence were compared by Fourier transform infrared (FTIR) analysis using a Digilab Model FTS 14 spectrophotometer (Rockwell International, Anaheim, California). Samples about 0.5 mm in width by 1.5 mm in length were placed on sodium chloride plates. The absorption spectra were constructed by co-adding 100 scans. Spectra for A240 pitch (AG 12-34) and the mesophase pitch (AG 164B) are compared in Fig. 4; spectra for three fractions from the mesophase pitch are compared in Fig. 5.

The spectra were analyzed primarily for their aliphatic and aromatic characteristics. The absorption bands¹¹ were assigned as follows:

- 3050 cm^{-1} = aromatic C-H stretching
- 2955 cm^{-1} = methyl C-H stretching
- 2920 cm^{-1} = methylene C-H stretching
- 2850 cm^{-1} = methyl C-H stretching
- 1600 cm^{-1} = aromatic C=C stretching
- 1450 cm^{-1} = methylene and methyl bending
- 1380 cm^{-1} = methyl bending
- 900 to 700 cm^{-1} = aromatic out-of-plane bending (primarily)

Table 3. Fractionation of A240 Petroleum Pitch AG 12-34

Fractionation Sequence AG 162-4					
Fraction	Hexane	Benzene	THF	Pyridine	Pyridine Insoluble
Fraction Depth, wt%	50.7	71.0	92.4	95.4	
Fraction Size, wt% ^a	50.7	20.3	21.4	3.0	4.6
Chemical Analysis, wt%					
Carbon	90.65	51.88	90.37	89.97	c
Hydrogen	5.87	5.04	4.89	4.61	c
Oxygen	1.00	0.70	3.18	b	c
Nitrogen	0.20	0.25	0.19	0.76	c
Sulfur	2.33	1.86	1.57	b	c
Ash	0.01	0.62	0.38	b	c
Atom Ratio, H/C	0.77	0.65	0.64	0.61	c
Coking Yield, wt%	42.1	70.3	75.5	84.6	c

^aFraction size equals fraction depth less depth of previous fraction.

^bInsufficient sample.

^cNot determined.

Table 4. Fractionation of Pyrolyzed Pitch AG 164A

Fractionation Sequence AG 162-5						
Fraction	Hexane	Chloroform	Benzene	THF	Pyridine	Pyridine Insoluble
Fraction Depth, wt%	46.6	90.1	91.2	92.4	95.4	
Fraction Size, wt%	46.6	43.5	1.1	1.2	3.0	4.6
Chemical Analysis, wt%						
Carbon	90.93	88.29	b	b	88.41	86.75
Hydrogen	5.86	5.20	b	b	4.71	3.89
Oxygen	1.01	5.15	b	b	3.51	b
Nitrogen	0.20	0.17	b	b	0.92	0.42
Sulfur	2.10	1.60	b	b	1.31	b
Ash	0.32	0.28	b	b	1.18	b
Atom Ratio, H/C	0.77	0.70	b	b	0.64	0.53
Coking Yield, wt%	46.8	72.7	b	71.6	83.0	91.8

^aFraction size equals fraction depth less depth of previous fraction.

^bInsufficient sample.

Table 5. Fractionation of Mesophase Pitch AG 164B

Fractionation Sequence AG 162-6				
Fraction	Hexane	Benzene	Pyridine	Pyridine Insoluble
Fraction Depth, wt%	35.2	61.7	71.4	
Fraction Size, wt% ^a	35.2	26.5	9.7	28.6
Chemical Analysis, wt%				
Carbon	90.30	91.66	91.24	90.16
Hydrogen	5.73	5.02	4.40	4.23
Oxygen	0.65	1.58	1.88	3.27
Nitrogen	0.21	0.26	0.85	0.26
Sulfur	2.13	1.61	1.23	1.34
Ash	0.09	0.48	0.43	0.81
Atom Ratio, H/C	0.76	0.65	0.58	0.56
Coking Yield, wt%	38.0	77.0	74.0 ^b	92.8

^aFraction size equals fraction depth less depth of previous fraction.

^bPyrolysis cell overflowed because of strong bloating.

Table 6. Fractionation of Mesophase Pitch AG 164B

Fraction	Fractionation Sequence AG 162-7				
	Hexane	Cyclohexane	Benzene	Pyridine	Quinoline Insoluble
Fraction Depth, wt%	32.6	41.8	63.5	75.0	94.9
Fraction Size, wt% ^a	32.6	9.2	21.7	11.5	19.9
Chemical Analysis, wt%					
Carbon	90.20	91.64	91.82	91.18	89.07
Hydrogen	5.74	5.47	5.08	4.45	3.53
Oxygen	0.51	0.62	1.52	2.02	1.48
Nitrogen	0.33	0.23	0.15	0.92	0.49
Sulfur	2.13	1.91	1.50	1.22	1.14
Ash	0.32	<0.10	0.31	0.13	3.75
Atom Ratio, H/C	0.76	0.71	0.66	0.58	0.47
Coking Yield, wt%	36.6	67.3	71.3	86.3	92.9

^aFraction size equals fraction depth less depth of previous fraction.

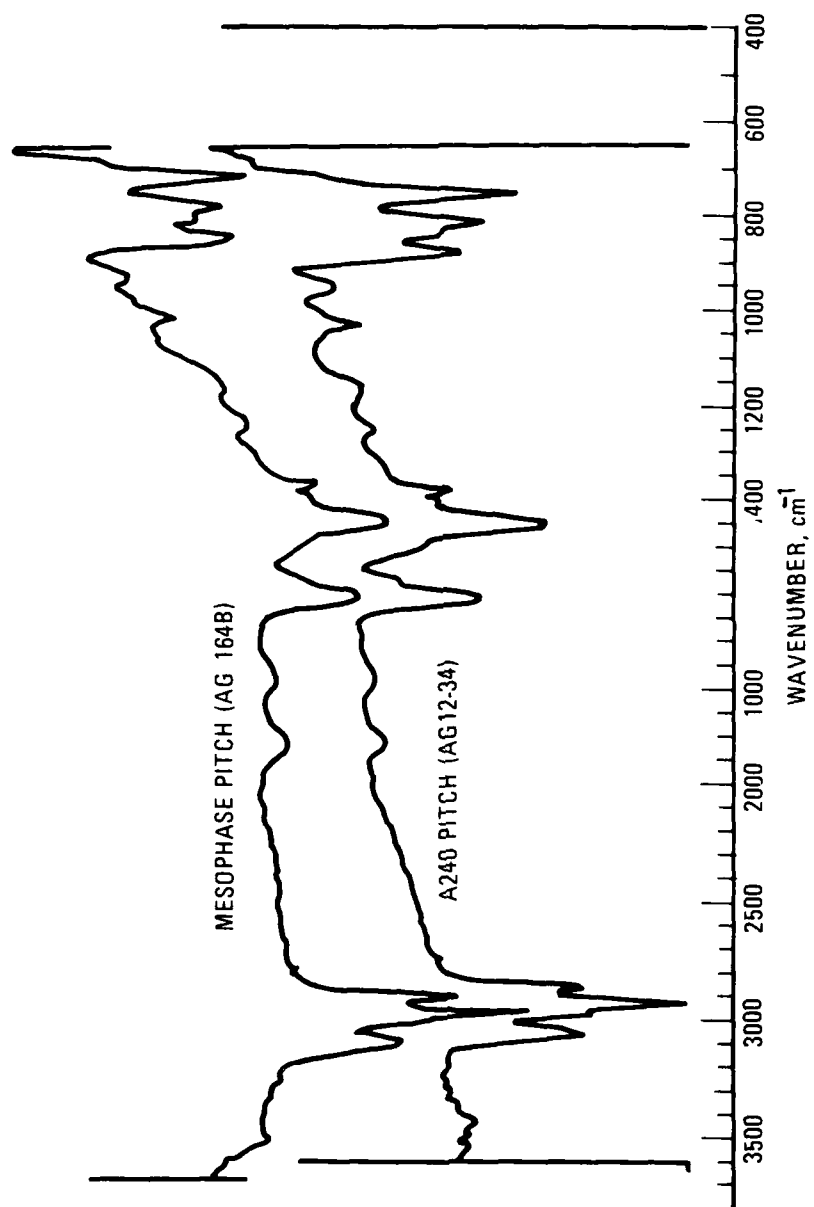


Fig. 4. Fourier Transform Infrared Spectra for A240 Petroleum Pitch
AG 12-34 and Mesophase Pitch AG 164B.

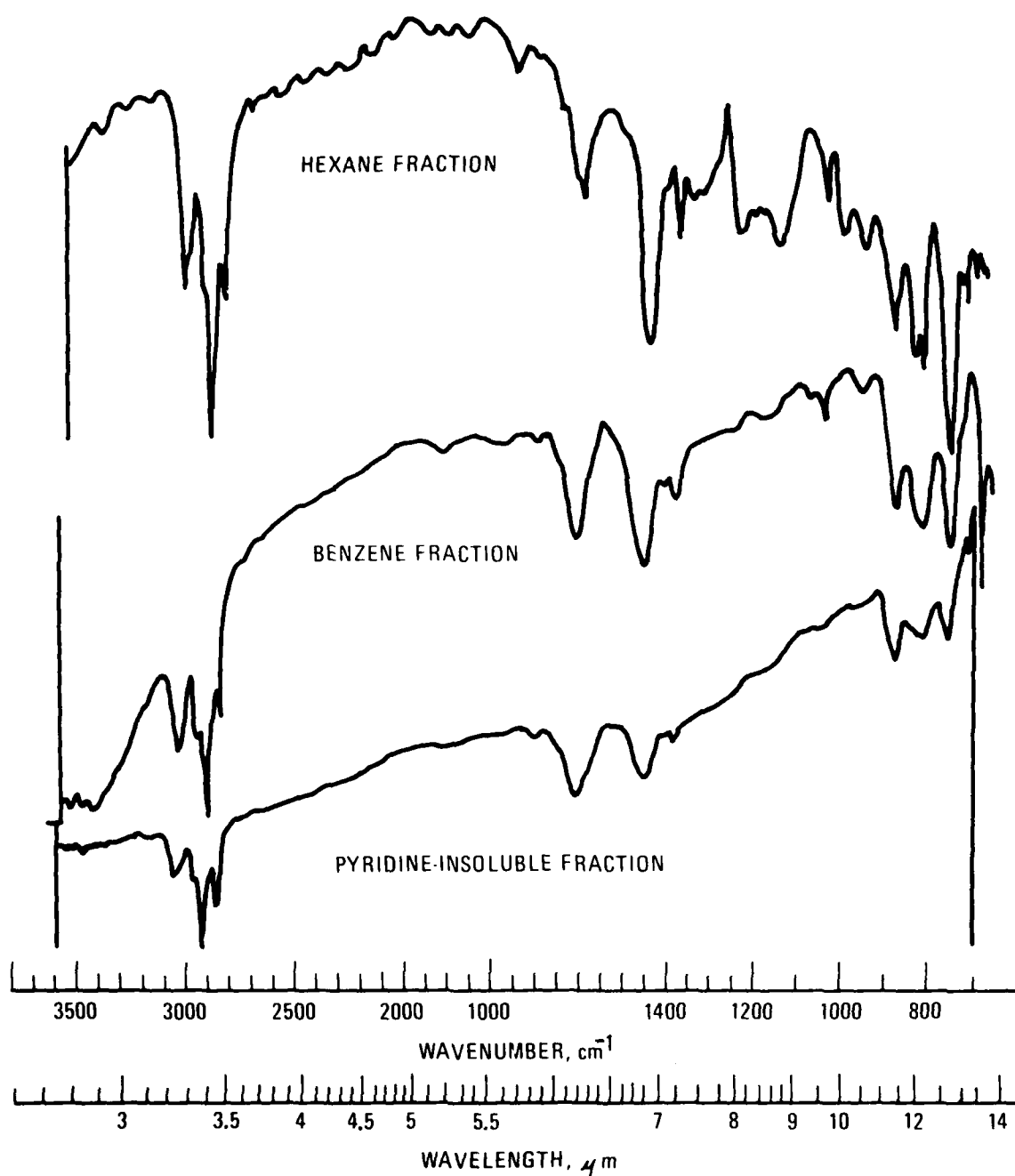


Fig. 5. Fourier Transform Infrared Spectra. Hexane, benzene, and pyridine fractions separated from mesophase pitch in fractionation series AG 162-7.

Absorption bands caused by oxygen-bearing functional groups should be small because the oxygen contents are moderate. The samples also contain some sulfur, but the absorption bands for sulfur-bearing functional groups are broad and weak;¹² possible contributions from sulfur-bearing groups were also ignored.

The aromatic and aliphatic characteristics of the sequence of fractions from the mesophase pitch were compared using the baseline method¹³ to estimate the absorbances at the aromatic peak (1600 cm^{-1}) and at the methyl-methylene peak (1450 cm^{-1}). The results are summarized in Table 7 in terms of the absorbance ratio. The thermal treatment of the A240 pitch causes some increase in aromatic character, but this increase is small relative to the differences effected by solvent fractionation. The absorbance ratio [$D_{\text{ar}}(1600\text{ cm}^{-1})/D_{\text{al}}(1450\text{ cm}^{-1})$] tends to increase regularly with depth of fraction. The plot of absorbance ratio as a function of H/C ratio (Fig. 6) shows a near-linear relationship; the quinoline fraction appears again as an exception that may be due to the thermal treatment necessary to vaporize the quinoline from the solute.

Table 7. Comparison of Aromatic and Aliphatic
Infrared Absorption Peaks

Pitch or Pitch Fraction	D_{ar} (1600 cm^{-1})	Atom Ratio, H/C
	D_{al} (1450 cm^{-1})	
A240 Petroleum Pitch (AG 12-34)	0.61	0.70
Mesophase Pitch (AG 164B)	0.72	0.66
Fractionation Sequence AG 162-7		
Hexane Fraction	0.36	0.76
Cyclohexane Fraction	0.61	0.71
Benzene Fraction	0.77	0.66
Pyridine Fraction	1.23	0.58
Quinoline Fraction	0.99	0.44
Pyridine-Insoluble Fraction	1.40	0.50
Quinoline-Insoluble Fraction	1.68	0.47

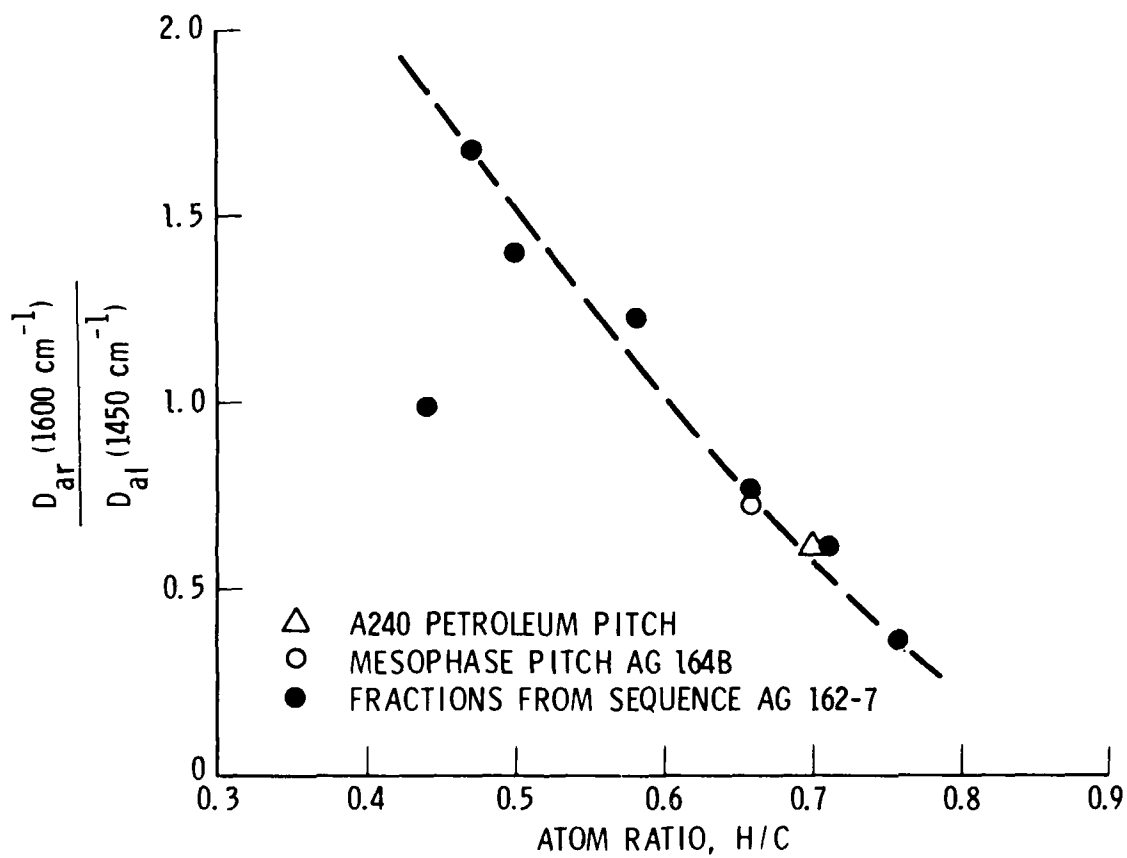


Fig. 6. Relative Aromaticities of Pitch Fractions as a Function of H/C Ratio. The ordinate is the ratio of absorbances at 1600 and 1450 cm^{-1} as measured from FTIR spectra.

III. PYROLYSIS OF PITCH FRACTIONS

Four sets of pitch fractions (AG 162-4 through -7) were pyrolyzed at room pressure in a programmed furnace with a large copper block to provide thermal inertia and temperature uniformity for simultaneous pyrolysis of 19 specimens. Slow heating was necessary to avoid excessive bloating; the block was heated at 13°C/hr to 360°C and then at 5°C/hr to reach the final coking temperature of 500°C.

The pyrolysis cell is illustrated in Fig. 7. An aluminum tube 19 mm in diameter by 76 mm high is shut by a close-fitting aluminum cap. The conditions for volatile release are fixed by a 0.5 mm pinhole and by loading each cell with the same mass (3 g). Nitrogen flowing through each cell at 15 liters/hr served as a protective atmosphere.

The coking yields given in Tables 1 and 3 through 6 are illustrated in Figs. 8 through 11. In general, the yield increases with the depth of the fraction, and the yields are approximately additive relative to the coking yield of the whole pitch.

All fractions bloated during pyrolysis except for the quinoline-insoluble fraction. The extents of bloating can be ranked by the level to which the foaming pitch rose during pyrolysis; the bloating behavior is given in parentheses for the various fractions of Figs. 8 through 11. In general, the bloating increased rapidly with the depth of the fraction until the insoluble fractions were reached.

PRECEDING PAGE BLANK-NOT FILMED

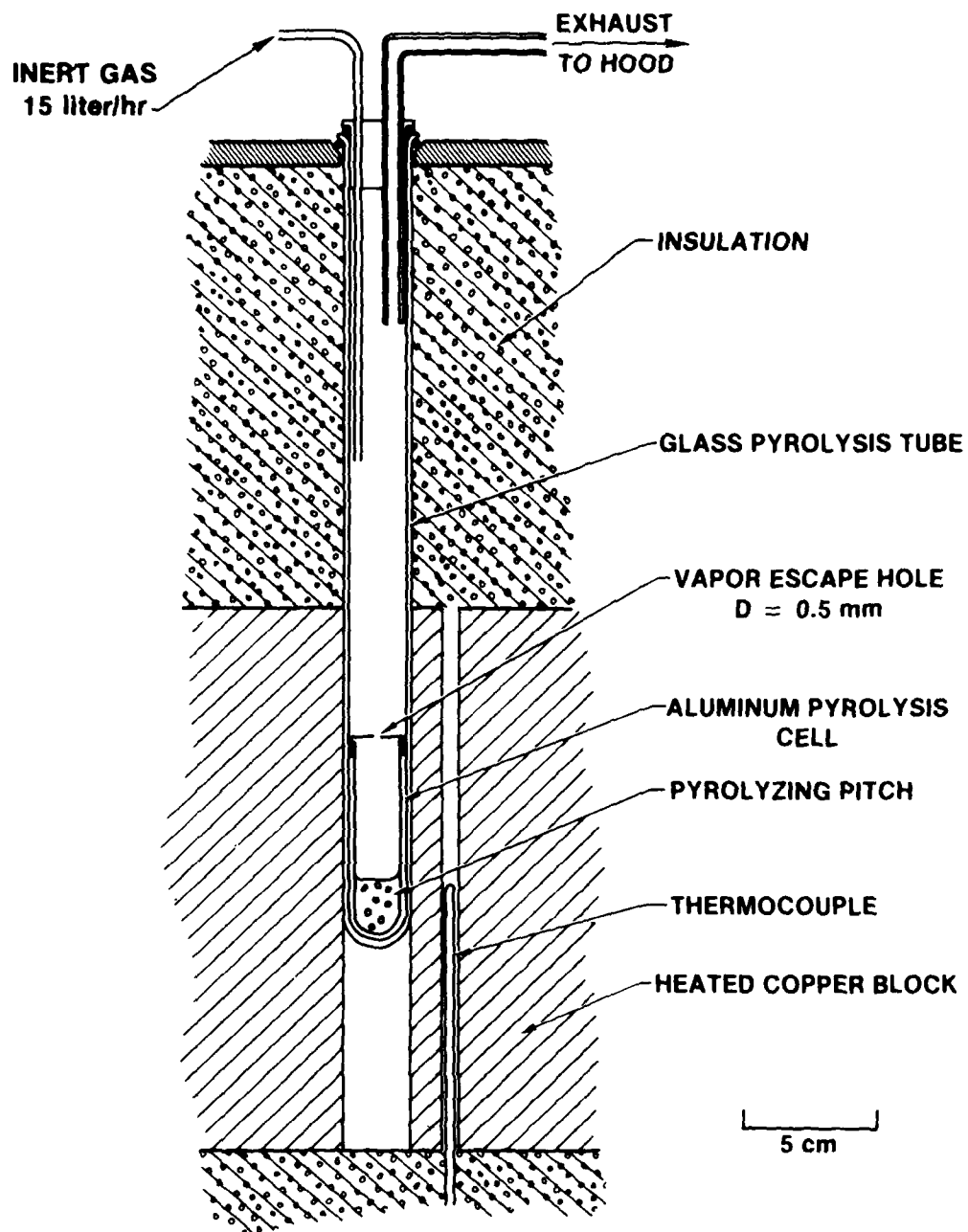


Fig. 7. Pyrolysis Cell. Copper block has 19 penetrations to accommodate glass tubes 25 mm in diameter.

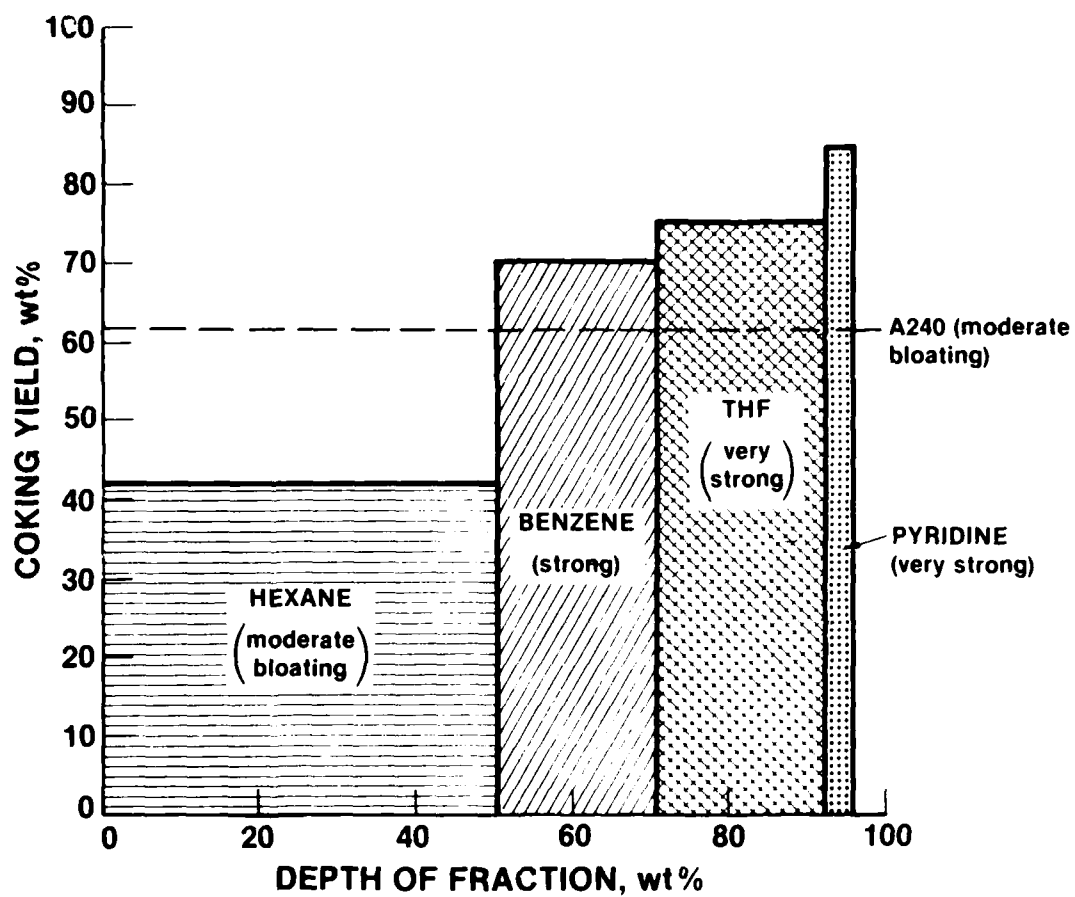


Fig. 8. Coking Yield and Bloating Behavior of Fractionation Sequence AG 162-4. Bloating behavior is noted in parentheses.

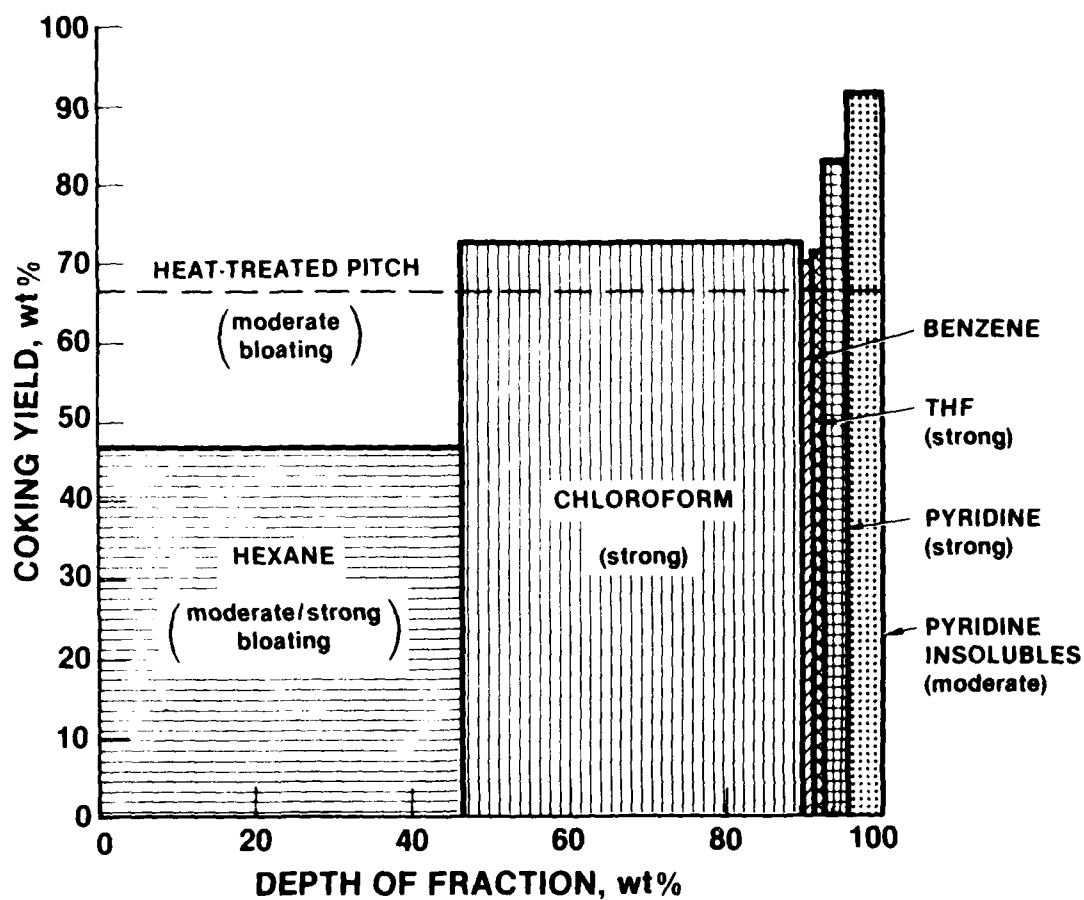


Fig. 9. Coking Yield and Bloating Behavior of Fractionation Sequence AG 162-5. Bloating behavior is noted in parentheses.

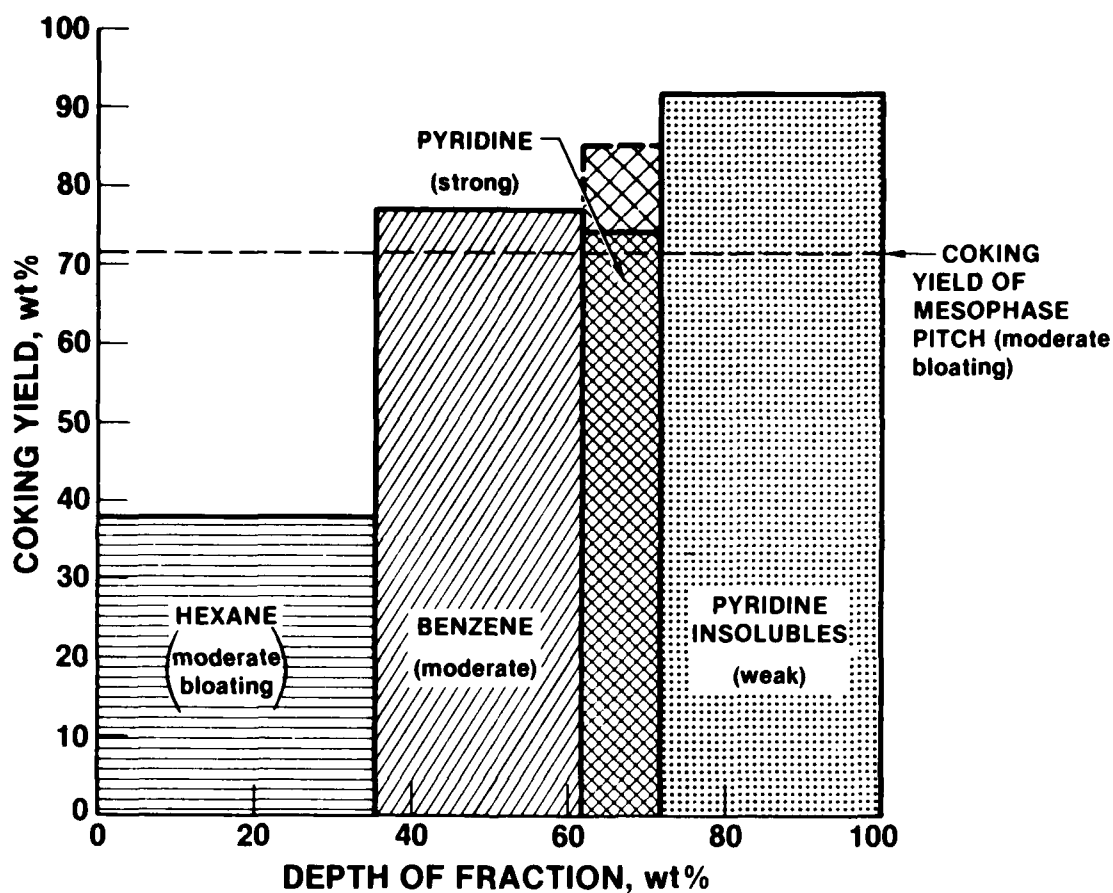


Fig. 10. Coking Yield and Bloating Behavior of Fractionation Sequence AG 162-6. Bloating behavior is noted in parentheses. The coking yield of the pyridine fraction is uncertain owing to some bloating overflow.

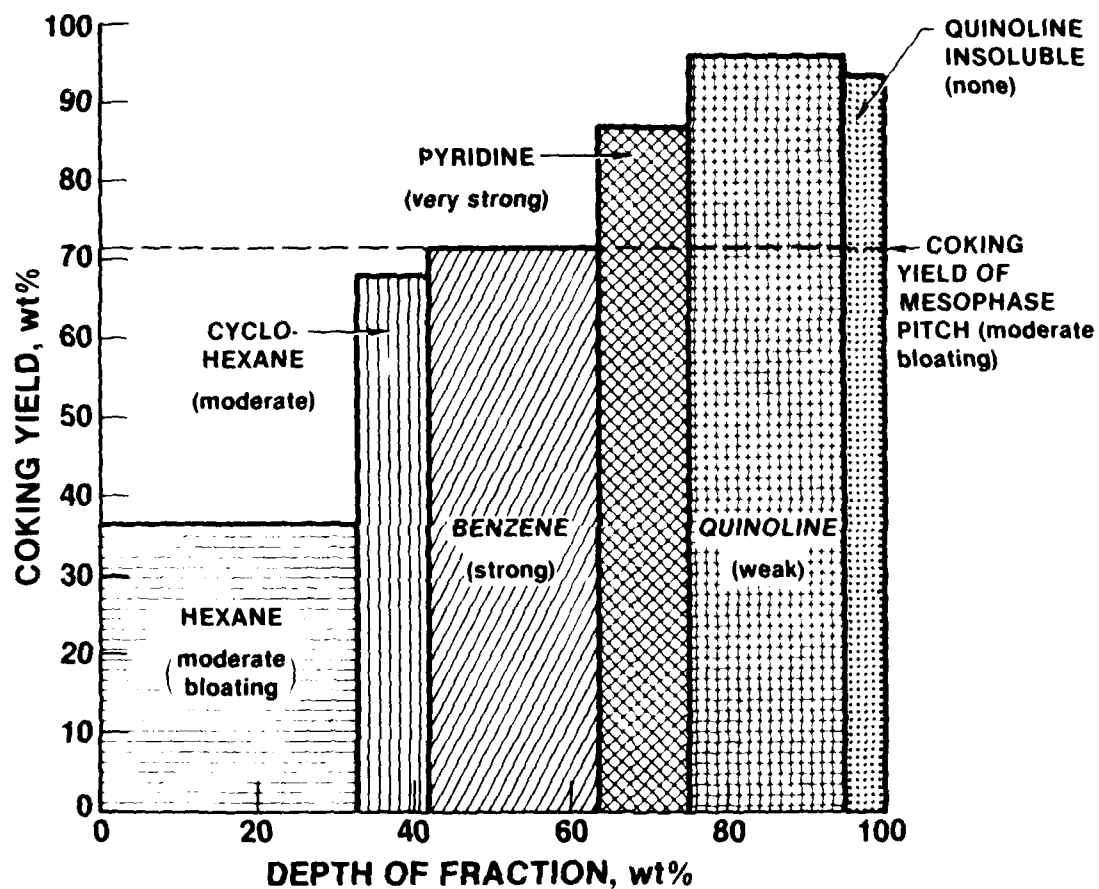


Fig. 11. Coking Yield and Bloating Behavior of Fractionation Sequence AG 162-7. Bloating behavior is noted in parentheses.

IV. MICROSTRUCTURES OF PYROLYZED FRACTIONS

The pyrolyzed fractions from fractionation series AG 162-4 through -7 were examined micrographically to (1) relate the microstructures to those from conventional cokes,⁵ (2) compare the microstructures from different fractions with those from the starting materials, and (3) obtain qualitative indications of the extent and effects of bloating during pyrolysis. Care was taken to examine full vertical sections to observe tendencies for microconstituents to be segregated.

Each pyrolysis residue was prepared for examination by mounting in a clear epoxy casting resin and cutting along the centerline of the pyrolysis cell to expose a full vertical section. Rough polishing was done with silicon carbide grinding paper (grits 320, 400, and 600). Fine polishing was done in three stages on a polishing wheel: (1) 9- μ m diamond paste (Diafin duPont diamond compound) on silk cloth (Buehler), (2) 1- μ m diamond paste on Texmet paper (Buehler), and (3) 0.05- μ m cerium oxide (Leco) on Microcloth (Buehler).

The microstructures of the four series of cokes were consistent in the sense that cokes derived from a given solvent showed similar structures and that these structures varied in nearly the same pattern through each fractionation series. Accordingly, microstructures are illustrated here for just two fractionation series: cokes from the fractionation series AG 163-5 (from the thermally treated pitch AG 164A) are examined individually at various magnification levels in Figs. 12 through 16, and cokes from the fractionation series AG 162-7 (from the mesophase pitch AG 164B) are compared in groups in Figs. 17 and 18.

A. FRACTIONATION SERIES AG 162-5

The starting material for the AG 162-5 fractionation sequence (Fig. 12) bloated moderately during pyrolysis to produce a coke with heavy bubble walls. Bubble percolation has produced some deformed microstructures, but the deformation does not approach the levels found in typical needle cokes.⁵ The structures illustrated in Fig. 12 were uniformly distributed over the vertical cross section.

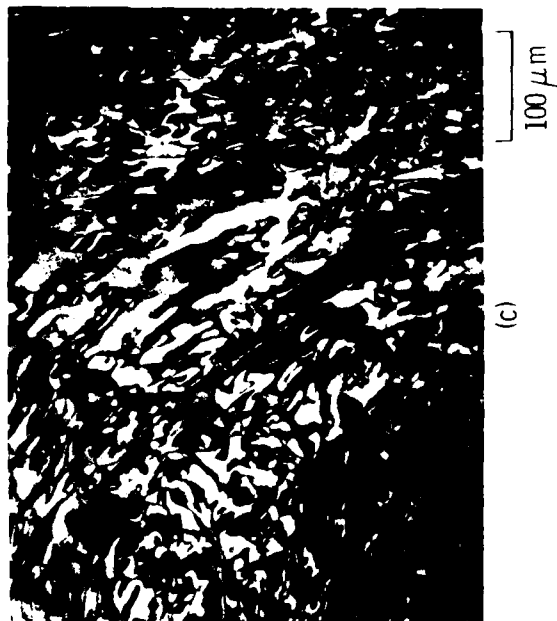
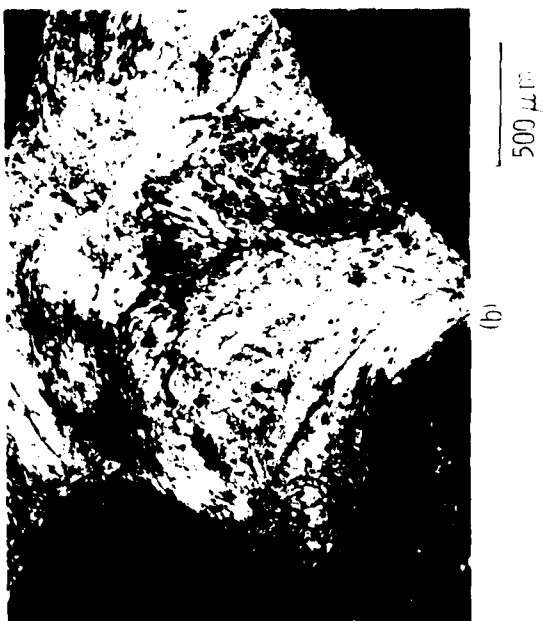


Fig. 12. Microstructure of Coke Formed by Pyrolysis of Pitch AC 164A. This pitch is the starting material for the fractionation series AC 162-5. Crossed polarizers. Views (b) and (c) are higher magnification views from (a).

The hexane fraction (Fig. 13) appeared to bloat more strongly, but the bubble walls are still relatively thick. The microstructures appear at two levels of coarseness. About 40% of the specimen appears in thick regions with a coarse undeformed structure (Fig. 13c); this microconstituent tends to occur in lower regions of the pyrolysis tube where deformation by bubble percolation is less likely. About 60% of the specimen appears in bubble walls with a fine structure reflecting a moderate level of deformation (Fig. 13b).

The chloroform fraction (Fig. 14) experienced strong bloating. The microstructure is primarily fine lamellar, typical of the bubble walls of a needle coke.⁵ This highly deformed microstructure formed despite an oxygen content in excess of 5 wt%.

The pyridine fraction (Fig. 15) bloated still more extensively; this effect is reflected in a finer, more lamellar microstructure.

The pyridine-insoluble fraction (Fig. 16) bloated only moderately. The majority of the specimen was glassy in microstructure, and nonresponsive to polarized light.

B. FRACTIONATION SERIES AG 162-7

The low magnification views of Fig. 17 demonstrate the rapid increase in bloating as the depth of fraction increases; this effect stops abruptly at the quinoline fraction. The higher magnification views of Fig. 18 show that the bloating behavior is paralleled by a steady refinement in the microstructural texture of the deformed microconstituents; this effect also stops abruptly at the quinoline fraction, where glassy microconstituents appear in the microstructure.

The coke produced from the mesophase pitch starting material displays a microstructure similar to many coal-tar pitch cokes (Ref. 4). Apparently some of the mesophase spherules produced in making the mesophase pitch have coked sufficiently hard to resist softening or melting in the pyrolysis to 500°C.

The hexane fraction, as well as the cyclohexane fraction, displays a duplex microstructure, with the coarser microconstituents found preferentially in the lower regions of the pyrolysis cells.

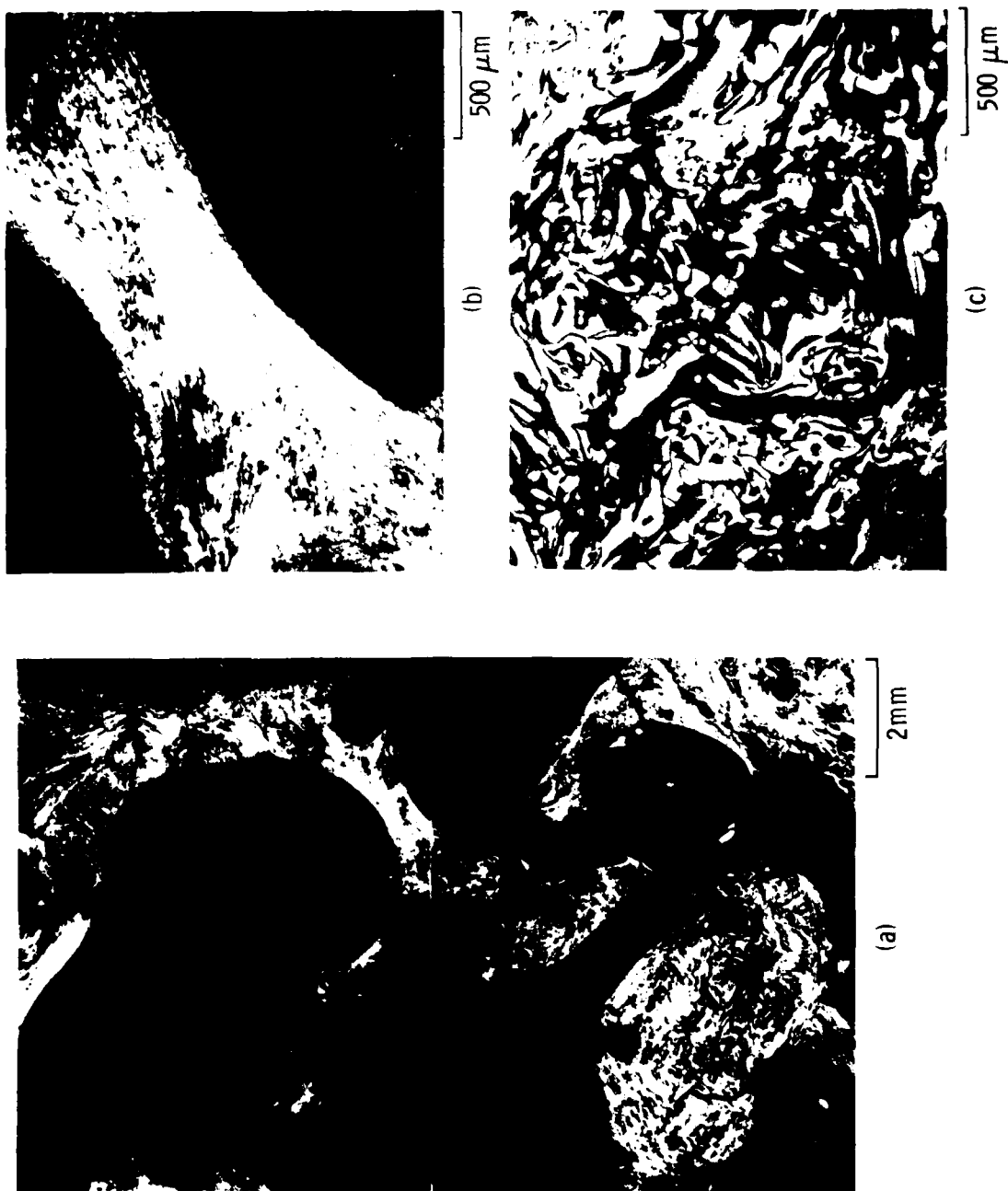


Fig. 13. Microstructure of Coke Formed by Pyrolysis of Hexane Fraction of Fractionation Series AG 162-5. Crossed polarizers. Views (b) and (c) illustrate fine- and coarse-structured regions of (a).

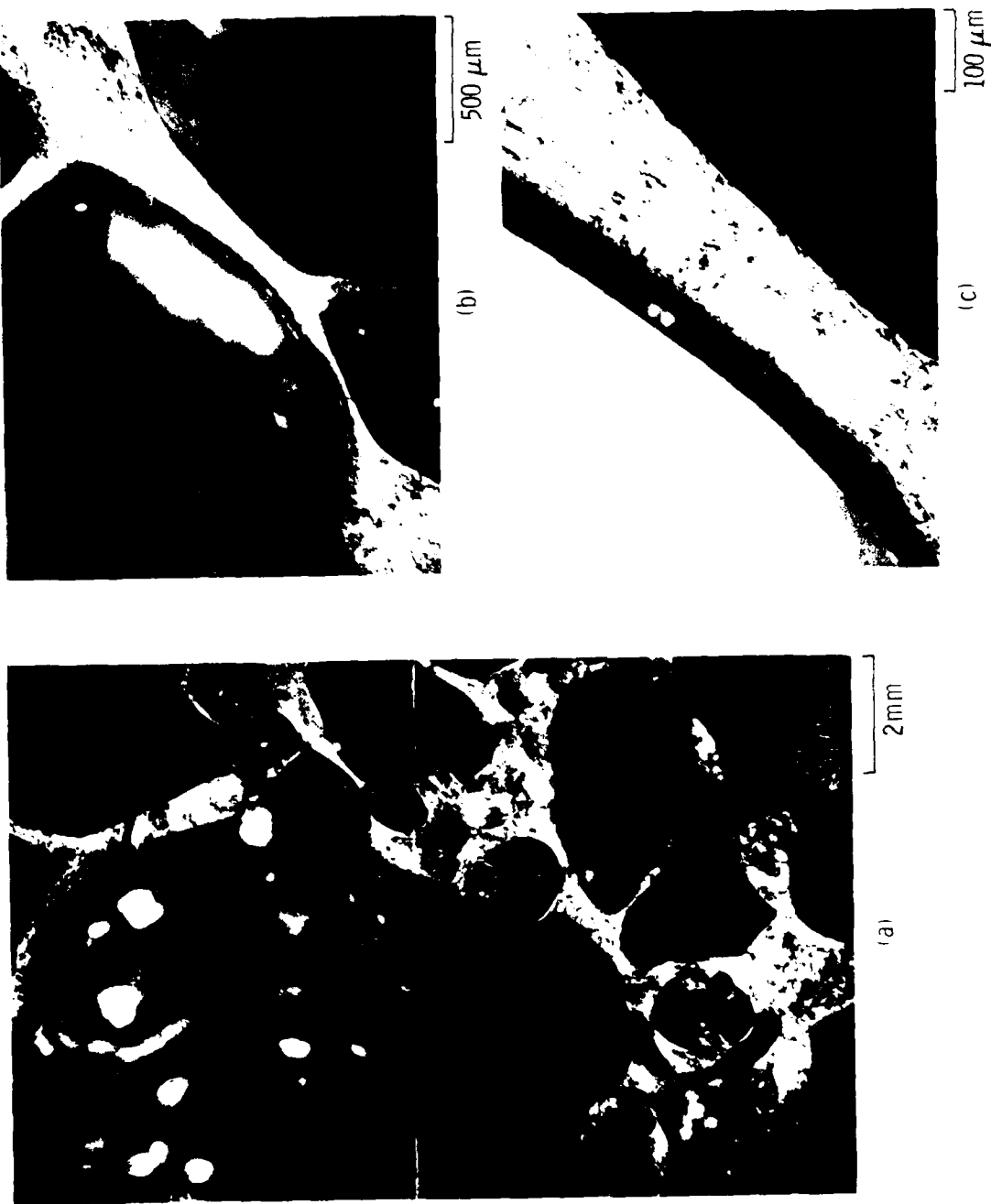
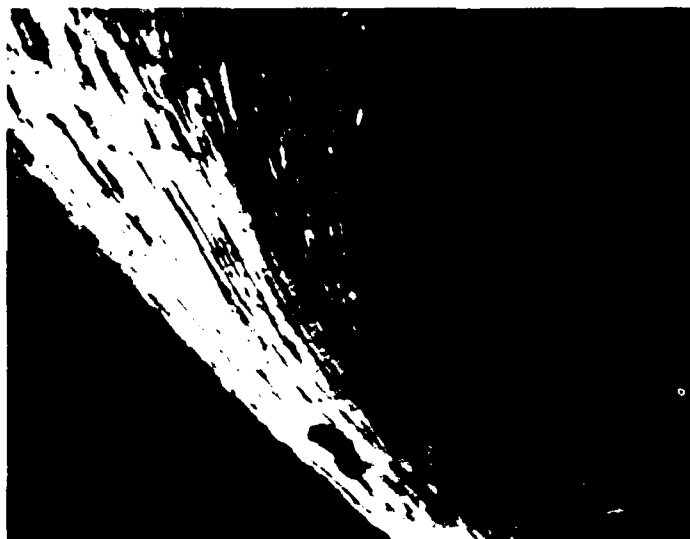


Fig. 14. Microstructure of Coke Formed by Pyrolysis of Chloroform Fraction of Fractionation Series AG 162-5. Crossed polarizers. Views (b) and (c) are higher magnification views of (a).



500 μm



100 μm

Fig. 15. Microstructure of Coke Formed by Pyrolysis of Pyridine Fraction of Fractionation Series AG 162-5. Crossed polarizers.



100 μm



50 μm

Fig. 16. Microstructure of Coke Formed by Pyrolysis of Pyridine-Insoluble Fraction of Fractionation Series AG 162-5. Polarized light.

Mesophase Pitch



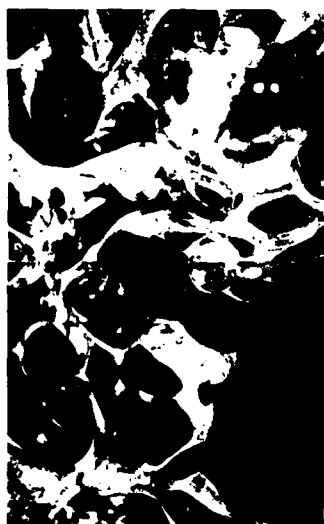
Hexane Fraction



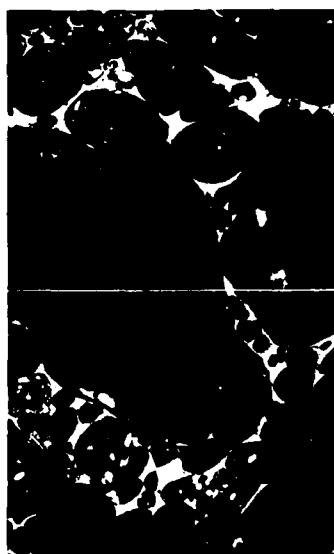
Cyclohexane Fraction



Benzene Fraction



Pyridine Fraction



Quinoline Fraction



Fig. 17. Microstructure of Cokes Produced by Pyrolysis of Fractions from Fractionation Series AG 162-7. Views at low magnification to illustrate differences in bloating behavior. Crossed polarizers.

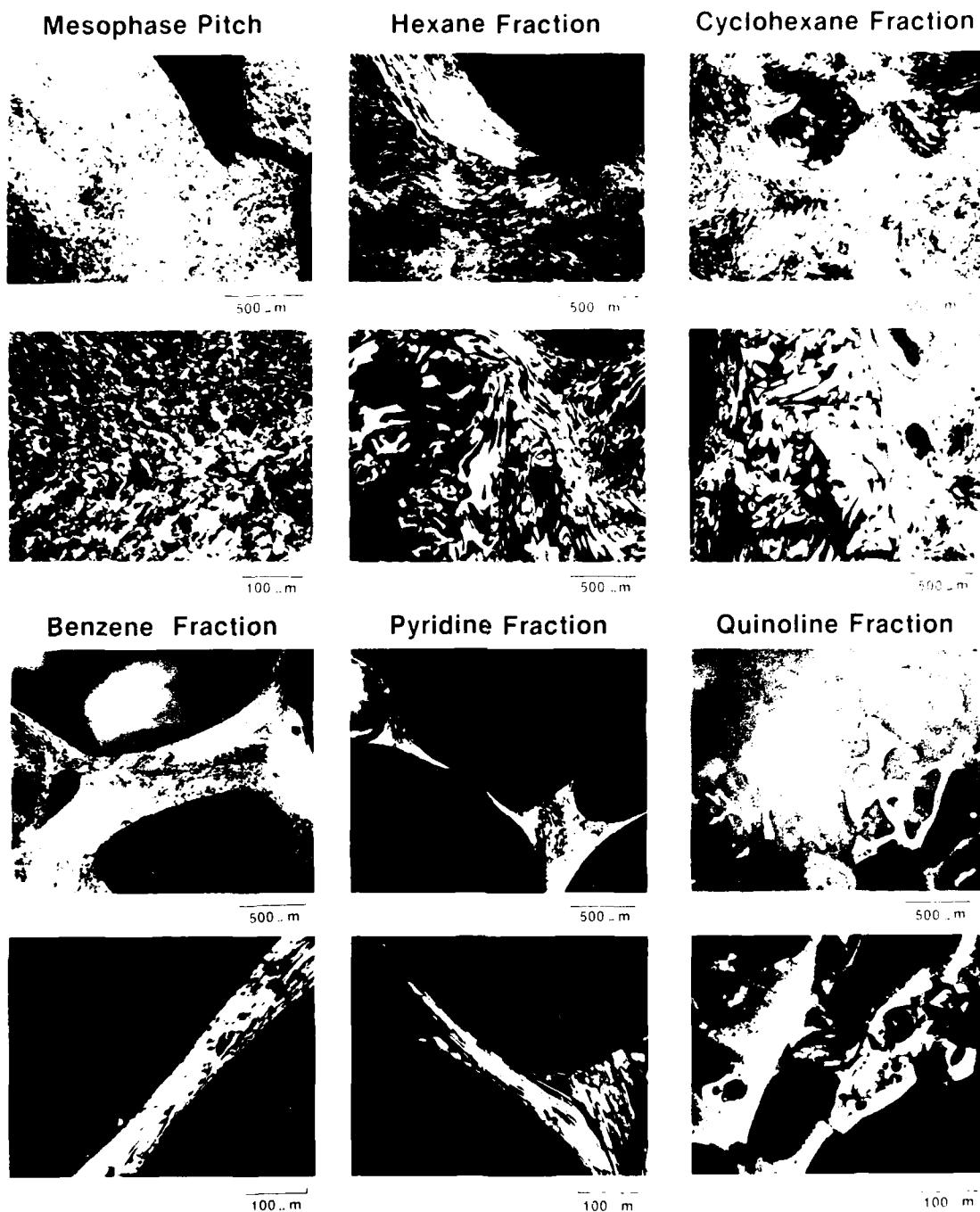


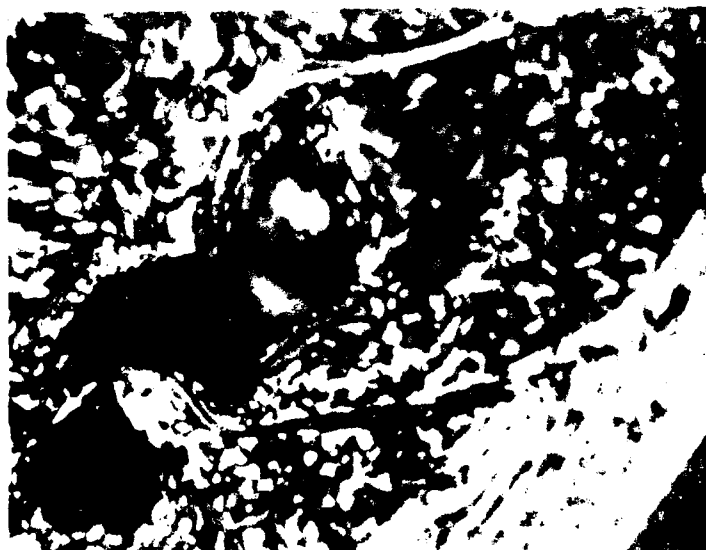
Fig. 18. Microstructure of Cokes Produced by Pyrolysis of Fractions from Fractionation Series AG 162-7. Views at higher magnification to illustrate differences in microstructure. Crossed polarizers.

The quinoline fraction showed an array of glassy and very fine-structured microconstituents; these are illustrated at the limit of optical resolution in Fig. 19.

The quinoline-insoluble fraction is shown at high magnification in Fig. 20. This nonbloating microstructure consists of mesophase spherules in a glassy matrix; these spherules, which appear to have hardened in the preliminary thermal treatment, actually constitute only a small fraction of the mesophase in the mesophase pitch.



50 μm

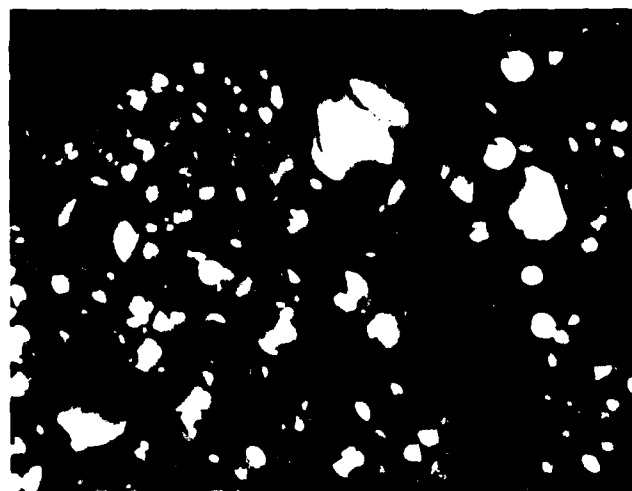


10 μm

Fig. 19. Microstructure of Coke Produced by Pyrolysis of Quinoline Fraction from Fractionation Series AG 162-7. Crossed polarizers.



500 μm



50 μm

Fig. 20. Microstructure of Coke Produced by Pyrolysis of Quinoline-Insoluble Fraction from Fractionation Series AG 162-7. Crossed polarizers.

V. DISCUSSION

The present results show that relatively simple fractionation procedures with increasingly aggressive solvents can be used to produce pitch fractions that vary appreciably but regularly in pyrolysis behavior. The chemical differences between the fractions are large relative to the changes that can be effected by thermal treatments applied to the whole pitches.

The pyrolysis behaviors of the four fractionation sequences that were studied in detail show consistent patterns of regular progression as the depth of the fraction increases; the pyrolysis yields and extents of bloating increase, while the microstructural textures become finer and eventually reach glassy microconstituents. The mesophase microstructures are similar to those observed in needle cokes,⁵ and the structural refinement appears to result from the deformation that the plastic mesophase experiences during bloating.

The bloating behavior may be significant to the performance of a pitch in composite processing because it offers a measure of the vulnerability of the mesophase to displacement from a matrix product by gas bubbles formed at critical stages of pyrolysis. In the present case, the bloating at room pressure increased with the depth of fraction despite the decrease in the H/C ratio. Note that bloating appears to depend not simply on the gas evolved in pyrolysis, but more precisely, on the gas evolved while the mesophase is in a plastic, deformable condition. Thus the extensive bloating of the deeper fractions may result from a large plastic range of the mesophase rather than an increase in the total gas evolution. Since the pyrolysis yield and bloating behavior display opposing effects with respect to the choice of promising candidate fractions for impregnation of carbon-carbon composites, further guidance should be sought in pyrolysis experiments at the pressures employed in composite fabrication. A test of bloating behavior under high pressure and at the scale of matrix pockets would appear most useful.

The analytical results in Tables 3 to 6 indicate that some fractions absorbed oxygen during the fractionation and solute-recovery procedures. No special precautions were taken to exclude air either during Soxhlet extraction

or in handling the powdered solute fractions. Although the microstructures of the pyrolyzed cokes, at least through to the pyridine-fraction, do not show serious effects of oxygen absorption, precautions should be taken in further work to blanket the Soxhlet system, as well as the powdered solutes, with an inert gas.

The pyrolysis behavior of the mesophase pitch reflects the range of molecular species present in the initial petroleum pitch. Some of the spherules present in the mesophase pitch, about 5%, appear to have hardened during the thermal treatment even though the pitch has reached only 50% transformation, and these spherules survive the sequential extractions to appear in nearly original condition in the pyrolysis of the quinoline-insoluble fraction (Fig. 20).

The solubilities of partially transformed pitches in pyridine or quinoline have been used in the past as measures of mesophase content on the assumption that these solvents are specific to the untransformed pitch. However, it may be observed from Fig. 3 that significant portions of the mesophase fraction of the mesophase pitch are soluble in quinoline, pyridine, and even benzene. The present results agree with the observations by Chwastiak and Lewis¹⁴ that some mesophase pitches, specially treated to avoid segregation and inhomogeneous polymerization, have substantial fractions of aromatic molecules large enough to precipitate as mesophase and small enough to dissolve appreciably in strong solvents.

REFERENCES

1. R. A. Greinke and L. H. O'Connor, "Determination of Molecular-Weight Distributions of Polymerized Petroleum Pitch by Gel Permeation Chromatography with Quinoline Eluent," Anal. Chem. **52**, 1877-81 (1980).
2. E. Fitzer, K. Mueller, and W. Schaefer, "The Chemistry of the Pyrolytic Conversion of Organic Compounds to Carbon," Chem. Phys. Carbon **4**, 237-383 (1971).
3. J. D. Brooks and G. H. Taylor, "The Formation of Some Graphitizing Carbons," Chem. and Phys. of Carbon **4**, 243-86 (1968).
4. J. L. White, "The Formation of Microstructure in Graphitizable Materials," Prog. in Solid-State Chem. **9**, 59-104 (1975).
5. J. L. White, "Mesophase Mechanisms in the Formation of the Microstructure of Petroleum Coke," in Petroleum-Derived Carbons, eds.; M. L. Deviney and T. M. O'Grady, Am. Chem. Soc. Symp. Series No. 21, 282-313 (1975).
6. G. R. Romovacek, "The Influence of Quinoline Insolubles on the Performance of Industrial Pitches," Carbon '80, 3rd Intl. Carbon Conf., 303-5 (1980).
7. S. Chwastiak, "Low Molecular Weight Mesophase Pitch," U.S. Patent 4, 209, 500 (24 June 1980).
8. K. L. Hoy, "New Values of the Solubility Parameters from Vapor Pressure Data," J. Paint Tech. **42**, 76-118 (1970).
9. A. F. M. Barton, "Solubility Parameters," Chem. Revs. **75**, 731-53 (1975).
10. D. M. Riggs and R. J. Diefendorf, "The Solubility of Aromatic Compounds," 14th Conf. on Carbon, Extended Abstracts, 407-8 (1979).
11. P. C. Painter, R. W. Snyder, M. Starsinic, M. M. Coleman, D. J. Kuehn, and A. Davis, "Concerning the Application of FTIR to the Study of Coal. A Critical Assessment of Band Assignments and the Application of Spectral Analysis Program," Technical Report, Pennsylvania State University, College of Earth and Mineral Sciences (1980).
12. M. St. C. Flett, Characteristic Frequencies of Chemical Groups in the Infra-red, Elsevier, New York (1963).

13. J. V. O'Gorman and P. L. Walker, Jr., "Mineral Matter and Trace Elements in U.S. Coal," Res. Dev. Rept. No. 61, Interim Rept. No. 2, Office of Coal Research, U.S. Dept. of Interior, Washington, D.C. (1972).
14. S. Chwastiak and I. C. Lewis, "Solubility of Mesophase Pitch," Carbon 16, 156-7 (1978).

LABORATORY OPERATIONS

The Laboratory Operations of The Aerospace Corporation is conducting experimental and theoretical investigations necessary for the evaluation and application of scientific advances to new military concepts and systems. Versatility and flexibility have been developed to a high degree by the laboratory personnel in dealing with the many problems encountered in the Nation's rapidly developing space systems. Expertise in the latest scientific developments is vital to the accomplishment of tasks related to these problems. The laboratories that contribute to this research are:

Aerophysics Laboratory: Aerodynamics; fluid dynamics; plasmadynamics; chemical kinetics; engineering mechanics; flight dynamics; heat transfer; high-power gas lasers, continuous and pulsed, IR, visible, UV; laser physics; laser resonator optics; laser effects and countermeasures.

Chemistry and Physics Laboratory: Atmospheric reactions and optical backgrounds; radiative transfer and atmospheric transmission; thermal and state-specific reaction rates in rocket plumes; chemical thermodynamics and propulsion chemistry; laser isotope separation; chemistry and physics of particles; space environmental and contamination effects on spacecraft materials; lubrication; surface chemistry of insulators and conductors; cathode materials; sensor materials and sensor optics; applied laser spectroscopy; atomic frequency standards; pollution and toxic materials monitoring.

Electronics Research Laboratory: Electromagnetic theory and propagation phenomena; microwave and semiconductor devices and integrated circuits; quantum electronics, lasers, and electro-optics; communication sciences, applied electronics, superconducting and electronic device physics; millimeter-wave and far-infrared technology.

Materials Sciences Laboratory: Development of new materials; composite materials; graphite and ceramics; polymeric materials; weapons effects and hardened materials; materials for electronic devices; dimensionally stable materials; chemical and structural analyses; stress corrosion; fatigue of metals.

Space Sciences Laboratory: Atmospheric and ionospheric physics, radiation from the atmosphere, density and composition of the atmosphere, aurorae and airglow; magnetospheric physics, cosmic rays, generation and propagation of plasma waves in the magnetosphere; solar physics, x-ray astronomy; the effects of nuclear explosions, magnetic storms, and solar activity on the earth's atmosphere, ionosphere, and magnetosphere; the effects of optical, electromagnetic, and particulate radiations in space on space systems.

FILMED

105-8